Ecosystems (2004) 7: 233–242
DOI: 10.1007/s10021-003-0189-x

ECOSYSTEMS

Remotely Sensed Interannual Variations and Trends in Terrestrial Net Primary Productivity 1981–2000

Mingkui Cao,* Stephen D. Prince, Jennifer Small, and Scott J. Goetz

Department of Geography, University of Maryland, LeFrak Hall, College Park, Maryland 20742-8225, USA

Abstract

Spatial and temporal variations in net primary production (NPP) are of great importance to ecological studies, natural resource management, and terrestrial carbon sink estimates. However, most of the existing estimates of interannual variation in NPP at regional and global scales were made at coarse resolutions with climate-driven process models. In this study, we quantified global NPP variation at an 8 km and 10-day resolution from 1981 to 2000 based on satellite observations. The high resolution was achieved using the GLObal Production Efficiency Model (GLO-PEM), which was driven with variables derived almost entirely from satellite remote sensing. The results show that there was an increasing trend toward enhanced terrestrial NPP that was superimposed on high seasonal and interannual variations associated with climate variability and that the increase was occurring in both northern and tropical latitudes. NPP generally decreased in El Niño season and increased in La Niña seasons, but the magnitude and spatial pattern of the response varied widely between individual events. Our estimates also indicate that the increases in NPP during the period were caused mainly by increases in atmospheric carbon dioxide and precipitation. The enhancement of NPP by warming was limited to northern high latitudes (above 50°N); in other regions, the interannual variations in NPP were correlated negatively with temperature and positively with precipitation.

Key words: net primary production; interannual variability; GLObal Production Efficiency Model (GLO-PEM); Advanced Very High Resolution Radiometer (AVHRR).

Introduction

Net primary production (NPP) quantifies the net carbon fixed by vegetation; in effect, it is the beginning of the carbon biogeochemical cycle. As a principal indicator of ecosystem health, resource utilization, and biospheric carbon fluxes, NPP is of great importance to ecological studies, natural resource management, and estimates of the terrestrial carbon sink. Terrestrial ecosystems drive most of the seasonal and interannual variations in atmospheric carbon dioxide (CO_2) concentration and have taken up about one-fifth of the total anthropogenic emission of CO_2 since the Industrial Revolution (Prentice and others 2001). Atmospheric measurements and inverse modeling suggest that the net terrestrial carbon uptake increased substantially from the 1980s to the 1990s (Battle and others 2000; Bousquet and others 2000), but the causes of the increase are not well understood (Schimel and others 2001). Quantifying variations in terrestrial NPP should provide insight into the processes and factors that regulate the terrestrial carbon sink.

Net primary production is highly variable in space and time. Spatial variations of NPP are related to factors such as climate, vegetation distribution, and land use across the planet from local to global scales. Temporal changes in NPP are linked to both

Received 15 May 2002; accepted 10 March 2003; published online 2 April 2004.
*Corresponding author; e-mail: mkcao@glue.umd.edu

"fast" processes (such as diurnal and seasonal variability in weather and the consequent physiological responses) and "slow" processes (such as changes in atmospheric composition, climatic changes, and ecosystem redistribution). Process-based ecosystem models have been widely applied as a means of quantifying spatio-temporal variations in NPP at large scales (for example, see Cao and Woodward 1998; Cramer and others 2001). However these models use a "scaling up" approach to extrapolate long-term estimates from short-term biological responses at small spatial scales; hence they often fail to correctly capture the long-term responses at large spatial scales. Moreover, process-based models are usually driven by meteorological data recorded at weather stations that are widely scattered and often sparse in number, particularly in the vast remote areas of the world. Therefore, the fine-resolution variation of NPP cannot be captured.

Satellite remote sensing provides information on vegetation patterns and activities at high resolution. For example, the Advanced Very High Resolution Radiometers (AVHRR) on board the National Ocean and Atmosphere Administration (NOAA) satellites have yielded global observations at a resolution of 1 km and 1–2 days for more than 20 years. Moreover, satellite observation can detect actual vegetation changes over large areas directly, hence avoiding the problems associated with "scaling up" in process modeling and the extrapolation of results from point measurements. Since 1984, when global observations of terrestrial vegetation were first made using the normalized difference vegetation index (NDVI) (Asrar and others 1984; Tucker and others 1985; Prince 1991a), various satellite-based techniques have been developed to measure vegetation changes. Many studies have used NDVI to estimate interannual changes in vegetation growth in an attempt to quantify the terrestrial carbon sink (for example, Myneni and others 1997, 2001; Zhou and others 2001; Tucker and others 2001). However, NDVI is not a direct measure of plant productivity or carbon uptake. In addition to the absorption of photosynthetically active radiation (PAR) by vegetation, which can be measured adequately with NDVI, NPP also depends on factors such as plant radiation utilization efficiency (RUE), which varies widely with the same NDVI (Prince 1991b; Goetz and Prince 1999).

To establish a link between satellite data and NPP, production efficiency models have been developed that estimate plant PAR absorption, RUE, and autotrophic respiration (Prince 1991b; Potter and others 1993; Prince and Goward 1995). These models have mostly been used to estimate spatial and seasonal patterns of NPP (Potter and others 1993; Prince and Goward 1995; Field and others 1998), but there have also been a few attempts to estimate interannual variation in NPP (Malmström and others 1997; Potter and others 1999; Behrenfeld and others 2001). However, those estimates used only NDVI from satellite data and still relied on coarse-resolution meteorological data from weather stations.

Environmental variables that affect RUE and autotrophic respiration, such as temperature and air humidity, can also be inferred from satellite data. Surface thermal energy emission detected by satellites has been used to infer temperature, humidity, soil moisture, and precipitation (Prince and Goward 1996; Rundquist and others 2000). To make use of the satellite data for estimating NPP, the GLObal Production Efficiency Model (GLO-PEM) was developed (Prince and Goward 1995). It was designed to run with both biological and environmental variables derived from satellites (Prince and Goward 1995; Goetz and others 2000); thus spatial and temporal variations of NPP can be estimated at the same resolution as satellite data. In this study, we used GLO-PEM and the NOAA/NASA Pathfinder AVHRR Land (PAL) Global Area Coverage (GAC) data at resolutions of 8 km and 10 days to estimate spatiotemporal variations in NPP from 1981 to 2000.

Methods

The GLObal Production Efficiency Model (GLO-PEM)

GLO-PEM consists of linked components that describe the processes of canopy radiation absorption, utilization, autotrophic respiration, and the regulation of these processes by environmental factors (Prince and Goward 1995; Goetz and others 2000):

$$NPP = \sum t[(S_t N_t)\varepsilon_g - R] \qquad (1)$$

where S_t is the incident PAR in time t; N_t is the fraction of incident PAR absorbed by the vegetation canopy (Fapar), calculated as a function of NDVI (Prince and Goward 1995; Goetz and others 1999); ε_g is RUE in terms of gross primary production; and R is autotrophic respiration calculated as a function of vegetation, biomass, air temperature, and photosynthetic rate (Prince and Goward 1995; Goetz and others 1999). The algorithms for calculating these variables are described in Prince and Goward (1995) and Goetz and others (1999). In this study, the estimate of ε_g was improved, as will be described in the following sections.

Plant photosynthesis depends on the efficiency of the photosynthetic enzyme system to assimilate CO_2 and the stomatal conductance of CO_2 diffusion into leaf intercellular spaces (Farquhar and others 1980; Collatz and others 1991). Therefore, ε_g is given as:

$$\varepsilon_g = \varepsilon_g^* \tilde{\sigma} \quad (2)$$

where ε_g^* is the maximum possible efficiency implied by photosynthetic biochemical processes that is affected by, among other factors, photosynthetic pathway, temperature, and the CO_2/O_2 specificity ratio (Prince and Goward 1995). σ is the reduction of ε_g^* caused by environmental factors that control stomatal conductance (Stewart 1988):

$$\sigma = f(T)\, f(\delta q)\, f(\delta\theta) \quad (3)$$

where $f(T)$, $f(\delta q)$, and $f(\delta\theta)$ represent the effects of air temperature, vapor pressure deficit (VPD), and soil moisture on stomatal conductance, respectively.

The temperature effect, $f(T)$, reaches the maximum (1.0) at the optimum temperature and tapers off for warmer or cooler temperatures (Raich and others 1991):

$$f(T) = \frac{(T - Tmin)(T - Tmax)}{(T - Tmin)(T - Tmax) - (T - Topt)^2} \quad (4)$$

where T is air temperature (°C); and *Tmin, Topt,* and *Tmax* are the minimum, optimum, and maximum temperatures (°C), respectively, for photosynthesis. We define the *Tmin* and *Tmax* as −1°C and 50°C for C_3 plants and 0°C and 50°C for C_4 plants, respectively (Parton and others 1993; Melillo and others 1993). The optimum temperature is defined as the long-term mean temperature for the growing season, based on the concept that plants grow efficiently at the prevailing temperature (Sellers and others 1992).

The water status of the leaf and soil are critical to stomatal conductance. As the air dries, stomata progressively close to protect the leaf from desiccation and so $f(\delta q)$ decreases (Jarvis 1976):

$$\begin{aligned} f(\delta_q) &= 1 - 0.05\delta_q \quad 0 < \delta_q <= 15 \\ &= 0.25 \qquad\qquad \delta_q > 15 \\ \delta_q &= Qw(T) - q \end{aligned} \quad (5)$$

where δ_q is the specific humidity deficit (g kg^{-1}), *Qw(T)* is the saturated specific humidity at the air temperature, and q is the specific humidity of the air. Soil moisture affects stomatal conductance through both hydraulic and nonhydraulic linkage between roots and leaves (Gollan and others 1992). Even if the water status of the leaf remains unchanged, stomatal conductance decreases with decreases in soil moisture in response to the resulting increases in abscisic acid in the roots (Tardieu and Davies 1993). The effect of soil moisture is given as:

$$f(\delta\theta) = 1 - \exp(0.081(\delta\theta - 83.03)) \quad (6)$$

where $\delta\theta$ is the soil moisture deficit (mm) in the top 1.0 m of soil. The soil moisture deficit is defined as the difference between saturated water content and actual water content, which is calculated with the algorithms described in Prentice and others (1992).

Satellite Data Sources and Processing

Pathfinder AVHRR Land (PAL) data at resolutions of 8 km and 10 days (Agbu and James 1994) were used to drive GLO-PEM. They were derived from channels 1, 2, 4, and 5 of the sensors aboard the NOAA -7, -9, -11, and -14. The PAL AVHRR data used in this study were reprocessed to incorporate corrections in the calculation of solar zenith angles and relative azimuth angles as well as corrections to remove atmospheric effects. The desert target approach (Rao 1993) was used to calibrate the data sets. GLO-PEM has algorithms to correct for cloud screening and water vapor Rossow and others 1996). As the NOAA satellites aged or changed, the equatorial crossing time changed significantly (Gutman 1999a). Therefore, data from channels 4 and 5 were corrected using a method that generally follows Gutman (1999a) but has major modifications (Gleason and others 2002).

GLO-PEM includes algorithms to calculate NDVI, Fapar, biomass, air temperature, and VPD from the AVHRR data (Prince and Goward 1995; Goetz and others 1999). The algorithms have been validated with field observational data (Goetz and others 1999; Prince and others 1998; Czajkowski and others 1997). The incident PAR was obtained from the International Satellite Cloud Climatology Project (ISCCP) (Pinker and Laszlo 1992; Frouin and Pinker 1995). The Global Precipitat Clmatology Project (GECP) version 2 combined a precipitation data set inferred from infrared and microwave satellites (Huffman and Bolvin 2000). Monthly atmospheric CO_2 concentrations came from the measurements of the Mauna Loa Station; these values are close to the means of the global observatory network (Keeling and Whorf 2002). The aerosol cloud released by the Pinatubo eruption in June 1991 covered over 40% of the planet (Robock 2002), preventing AVHRR from effective monitoring of land surface conditions to the end of 1992 (Gutman 1999b). Therefore, the estimate for the period from July 1991 to December 1992 was excluded from analysis.

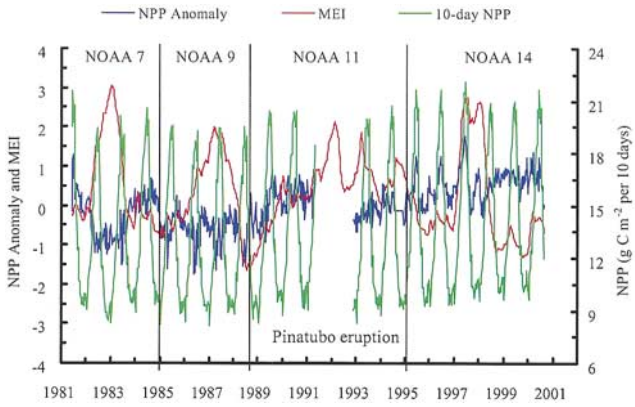

Figure 1. Temporal variation in net primary production (NPP) and its response to the ENSO cycle. The NPP anomaly (g C m^{-2} $10d^{-1}$) was calculated as a deviation from the mean in the period 1981–2000. The multivariate ENSO index (MEI) is positive for El Niño and negative for La Niña.

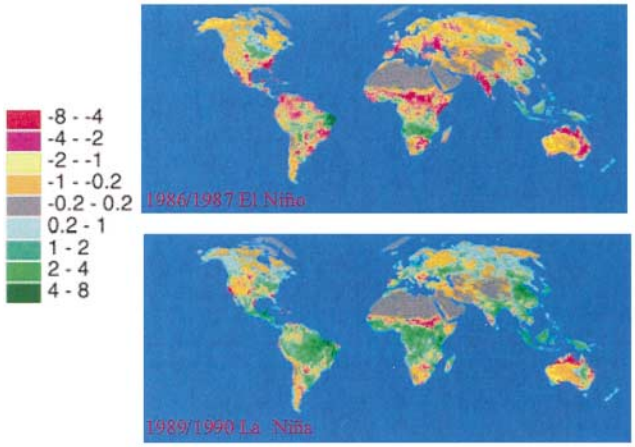

Figure 2. Anomalies in net primary production (NPP) (g C m^{-2} $10d^{-1}$) estimated for a typical El Niño and La Niña episode as a deviation from the mean in the period 1981–2000.

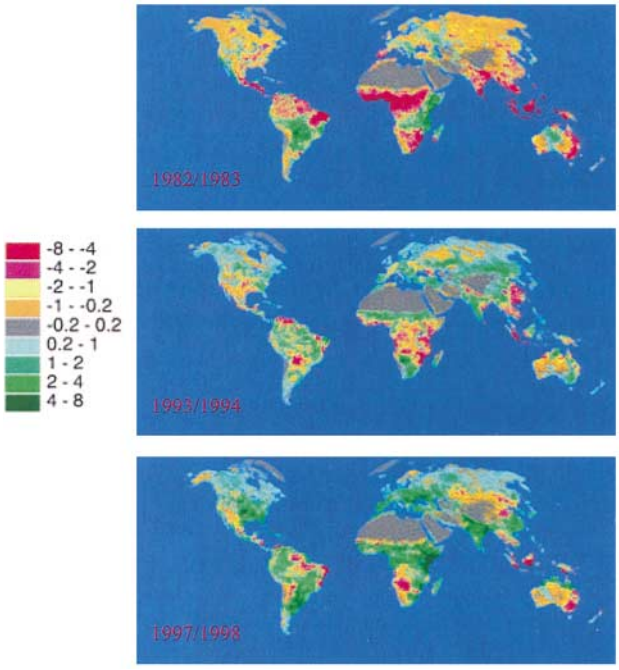

Figure 3. Varying responses of net primary production of (NPP) to different El Niño events. The NPP anomaly (g C m^{-2} 10 d^{-1} is the deviation from the mean for the period 1981–2000. The spread of aerosols from the Chichón eruption in Mexico in 1982 might have affected the estimate of NPP changes in 1982–83 at low latitudes, but the global NPP reduction, particularly in the north, was caused mainly by the strong El Niño.

Results

Global Interannual Variation in Net Primary Production

During the period 1981–2000, global NPP varied greatly from 8 to 22 g C m^{-2} 10 d^{-1} with a coefficient of variation (CV) of 28%. However, the deseasonalized interannual anomaly showed an increasing trend by 0.52% y^{-1} ($R^2 = 0.67$, $P < 0.01$) (Figure 1). The interannual variation in NPP was clearly correlated with the El Niño–Southern Oscillation (ENSO) cycle, which creates an alternation of dry and warm El Niño episodes, with wet and cool episodes over large parts of the tropics, and strongly affects the climate of other regions through teleconnections (Ropelewski and Halpert 1987; Glantz and others 1991). NPP generally decreased in El Niño episodes and increased in La Niña episodes (Figures 1 and 2). The global mean NPP for El Niño seasons, defined as the period when the multivariate ENSO index (MEI) was above 0.5 (Wolter and Timlin 1998) (Figure 1), was 3.6% lower than that for La Niña seasons, and the reduction was up to 10% in strong El Niño events, such as the ones that occurred in 1982–83 and 1986–87 (Figure 1).

In El Niño seasons, severe drought spread over Indonesia, the Philippines, northern South America, Central America, northern and southern Africa, India, and Australia, whereas warmer than normal conditions were found along the west coast of South America, southeastern Asia, and southern Africa (Ropelewski and Halpert 1987; Halpert and Ropelewski 1992; Moron and Ward 1998). For these regions, our estimated NPP dropped by about 8% in El Niño seasons (Figures 2 and 3). The strongest connections between El Niño and NPP reduction were found in India, northeastern South America, and eastern Australia (Figures 2 and 3),

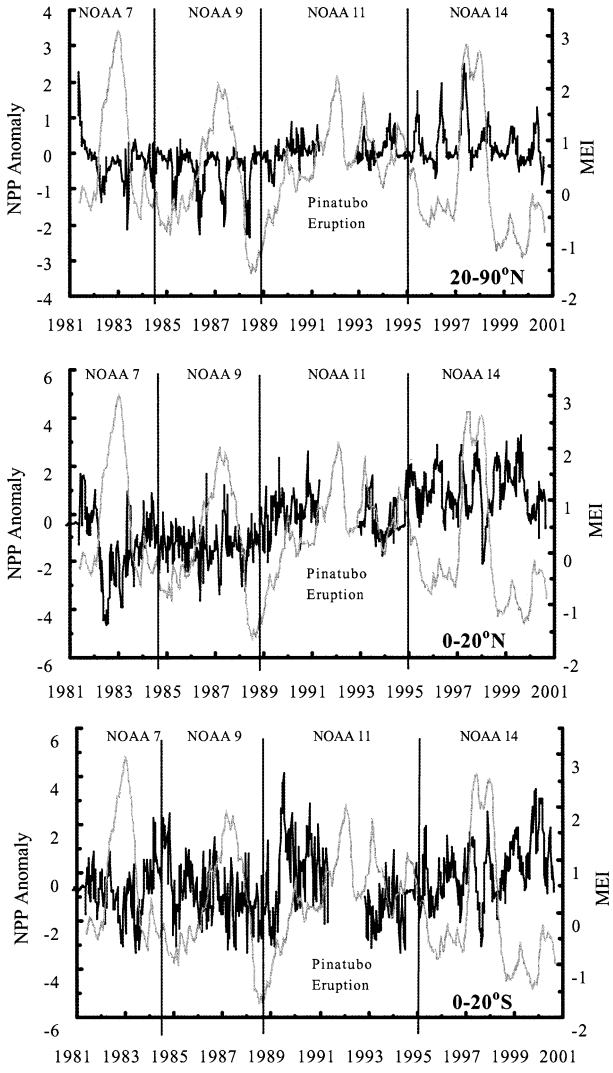

Figure 4. Interannual anomalies in net primary production (NPP) (g C m^{-2} $10d^{-1}$) for various latitudinal bands. The anomaly is a deviation of NPP from the mean in the period 1981–2000.

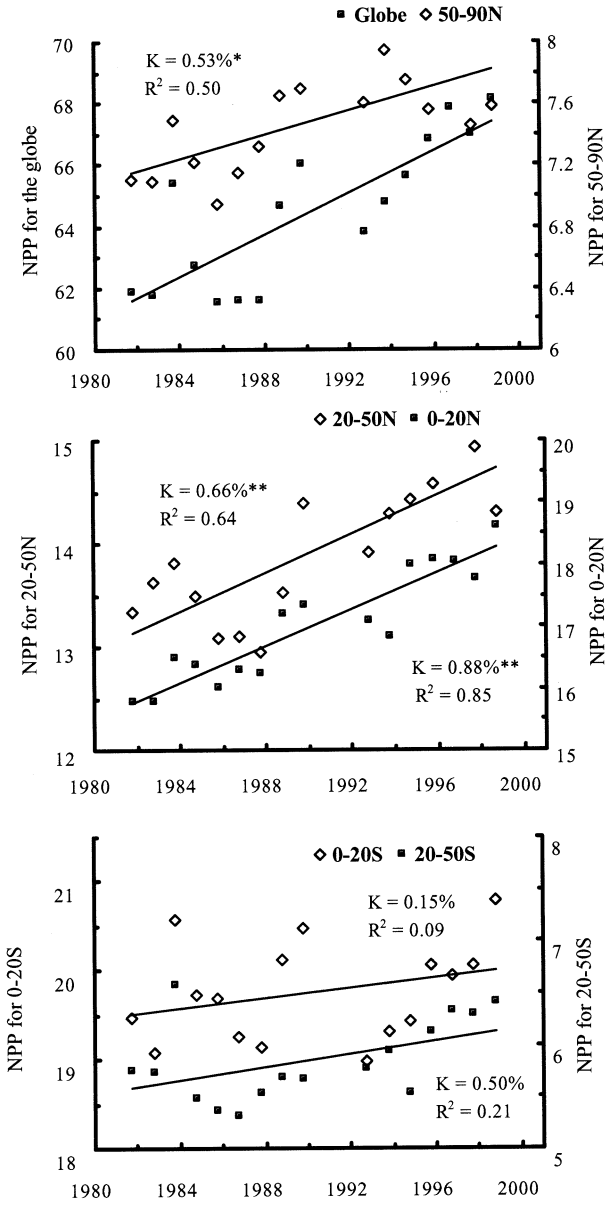

Figure 5. Estimated changes in annual total terrestrial net primary production (NPP) (Gt C) in various latitudinal bands and on a global basis. K represents the annual growth rate. A single asterisk (*) indicates that the estimated K was significant at a 95% level; a double asterisk (**) indicates that it was significant at a 99% level.

because the El Niño events suppressed the monsoon and greatly reduced precipitation in these regions (Dai and Wigley 2000). In the 1982–83 and 1986–87 El Niño seasons (Figures 2 and 3), NPP in India, northeastern South America, southern Africa, and the sub-Sahara fell by up to 20%.

Variations by Latitudinal Bands and Regions

Interannual variations in NPP had different characteristics in different regions (Figures 4 and 5). In the tropics (20°N–20°S), NPP increased by 0.48% y^{-1} ($R^2 = 0.59$, $P < 0.01$) during the study period. The anomalies in NPP were significantly correlated with MEI ($R^2 = 0.36$, $P < 0.01$) (Figure 4). The mean temperature increased by 0.46°C, precipitation fell by 8%, and NPP was reduced by 4% during El Niño seasons. In the north (higher than 20°N), NPP increased by 0.57% ($R^2 = 0.67$, $P < 0.01$). The interannual anomalies in NPP had no significant correlation with the MEI (Figure 4), but NPP still decreased in El Niño. The impact was substantial in some regions—for example, North America (Fig-

ures 2 and 3). The estimated NPP for North America decreased in El Niño seasons ($R^2 = 0.39$, $P < 0.01$), particularly in the central and southwestern United States, where severe warming and drought often occurred in El Niño seasons (Ropelewski and Halpert 1986; Wilhite and others 1987). In contrast, the NPP for Eurasia was not reduced significantly in El Niño seasons.

Although there are some consistent climate patterns associated with the ENSO cycle, individual events may have variable effects on climate and hence on NPP. In spite of the general drying effect, El Niño events often bring heavy rainfall to certain arid regions (Poliss and others 1997; Gutièrrez 2000). For example, precipitation in southern California and the arid interior of Australia in the 1982–83 El Niño season was respectively, 17% and 9% higher than the average, and estimated NPP increased by 5–10% (Figure 3). However, NPP in the same regions decreased in the 1986–87 El Niño season (Figure 2) due to reductions in precipitation. In contrast to the 1982–83 and 1986–87 El Niño events, which caused global reductions in NPP, the main impacts of the 1993–94 El Niño was limited to central Africa and the Asian Pacific, and the NPP in northern middle and high latitudes increased due to higher than normal precipitation (Figure 3).

In the transition from the 1987–88 El Niño to the 1988–89 La Niña, global NPP was still low (Figure 1) because precipitation did not return to normal levels and temperatures remained higher than normal in the middle and eastern United States, South America, central Africa, and Southeast Asia. The 1997–98 El Niño was probably the strongest one in the 20th century (Davey and Anderson 1999; Parker and others 1998); however, estimated NPP was only moderately reduced by this episode (Figure 1). The 1997–98 El Niño event, as usual, caused drought over eastern Brazil, southwestern Africa, and northeastern South America (Parker and Horton 1999; Slingo 1999); hence, there were marked reductions in NPP in these regions (Figure 3). However, the Indian monsoon rainfall was not reduced, and the eastern regions of Africa and the United States, southern South America, and western Europe experienced exceptionally wet weather (Slingo 1999; Lau and Wu 1999); thus, the estimated NPP for these regions was higher than normal (Figure 3). An independent estimate, using data from the Sea-viewing Wide Field-of-view Sensor (SeaWiFS) on the SeaStar spacecraft, also did not detect significant decreases in NPP for the 1997–98 El Niño (Behrenfeld and others 2001).

During the period 1981–2000, NPP generally increased in the Northern Hemisphere but showed no clear trend in the Southern Hemisphere (Figure 5). During the 1980s, NPP increased at northern high latitudes (above 50°N) by 0.71% y^{-1} ($R^2 = 0.40$, $P < 0.01$) and low latitudes (0–20°N) by 0.78% y^{-1} ($R^2 = 0.66$, $P < 0.01$), but it varied greatly between years in other latitudinal regions. In the 1990s (after 1992), NPP increased in almost all latitudinal bands, but the growth rate in the tropics—0.91% y^{-1} ($R^2 = 0.36$, $P < 0.01$)—was about twice that in the north (0.42% y^{-1}, $R^2 = 0.25$, $P < 0.01$). NPP showed a higher growth rate (0.48% y^{-1}, $R^2 = 0.38$, $P < 0.05$) in Eurasia than in North America (0.36% y^{-1}, $R^2 = 0.26$, $P < 0.05$) in the period 1981–2000.

Responses to Climate Variation

In the north (above 20°N), the mean annual temperature increased by 0.45°C and precipitation increased 12 mm in the study period. Interannual variation in NPP correlated positively with temperature ($R^2 = 0.21$, $P < 0.05$) in the northern high latitudes (above 50°N) but not in the middle latitudes (20–50°N), where NPP was positively correlated with precipitation ($R^2 = 0.25$, $P < 0.05$). In the tropics (20°N–20°S), the mean annual temperature increased by 0.32°C and precipitation increased 22 mm in the study period. NPP responded negatively to temperature ($R^2 = 0.33$ for the latitudinal band 0–20°N and 0.48 for 0–20°S, $P < 0.01$) and positively to precipitation ($R^2 = 0.57$ for 0–20°N and 0.38 for 0–20°S, $P < 0.01$). The atmospheric CO_2 concentration increased 28 ppmv from 1981 to 2000. NPP was correlated with the increase in atmospheric CO_2 in all regions, with a correlation coefficient higher than 0.50. The response of photosynthetic biochemical reactions to increases in atmospheric CO_2 is higher under warmer conditions (Long 1991; Kirschbaum 1994), so the CO_2 fertilization effect is expected to increase with warming in cool regions and to be the greatest in warm environments. In addition, increases in atmospheric CO_2 can also enhance NPP by reducing stomatal conductance and increasing plant water-use efficiency, particularly in arid regions (Drake and others 1997; Körner 2000). According to the analysis, the warming trend enhanced NPP in northern high latitudes, increases in precipitation helped to enhance NPP in the northern middle latitudes and the tropics, and increases in atmospheric CO_2 contributed to NPP increases in all regions. Because northern high latitudes (above 50°N) accounted for only about 12% of the estimated global NPP, the global increase in NPP was mainly related to increases in atmospheric CO_2 and precipitation.

Comparisons with Studies Using other Methodologies

Our estimated increases of NPP in the north are supported by atmospheric measurements (Keeling and others 1996; Braswell and others 1997). In addition, the increases in the tropics are also consistent with documented observations (Phillips and others 1998) and process-based modeling (Grace and others 1995; Tian and others 1998). Studies based on atmospheric measurements and models found no significant carbon releases from tropical regions (Keeling and others 1996; Bousquet and others 2000), suggesting that increases in NPP counterbalance the carbon release caused by deforestation (Malhi and Grace 2000; Schimel and others 2001). Our estimate did not show a clear trend toward increasing NPP in the 1980s, due to high interannual variation; however, the authors of other satellite-based studies (Malmström and others 1997; Potter and others 1999) reported that global NPP had increased by more than 10% (but they gave no explanation for such large increases). Our estimates of increased NPP are in accord with the results of studies that used NDVI directly as an index of plant growth, but they contradict their hypothesis that warming drove the increase in the north (Zhou and others 2001; Lucht and others 2002). Our analysis showed that warming enhanced NPP in the northern high latitudes but not in the northern middle latitudes, where plant growth may decrease with warming because of concomitant water stress (Barber and others 2000); thus, our estimated NPP increases for this region were correlated with increases in precipitation.

The interannual variations and trends in NPP reflected in our estimates are in accord with the results yielded by a process-based biogeochemical model (Cao and Woodward 1998; Cao and others 2002) (Figure 6). Both of these methodologies produced similar findings of interannual variation ($R^2 = 0.41$, $P < 0.01$); indeed, our estimated NPP increase of 4.9% from the 1980s to 1990s is very close to the estimate of 3.5% produced with CEVSA (Cao and others 2002). Our estimate of NPP increases in the 1990s is also in line with the findings of other studies using atmospheric measurements and inverse modeling that suggested a substantial increase in net terrestrial carbon uptake in the 1990s (Battle and others 2000; Bousquet and others 2000). Our estimated response of NPP to ENSO cycles is further supported by atmospheric measurements that showed decreases in terrestrial carbon uptake in El Niño seasons and increases in La Niña seasons (Keeling and others 1996; Keeling and Whorf 2002; Bousquet and others 2000) (Figure 7).

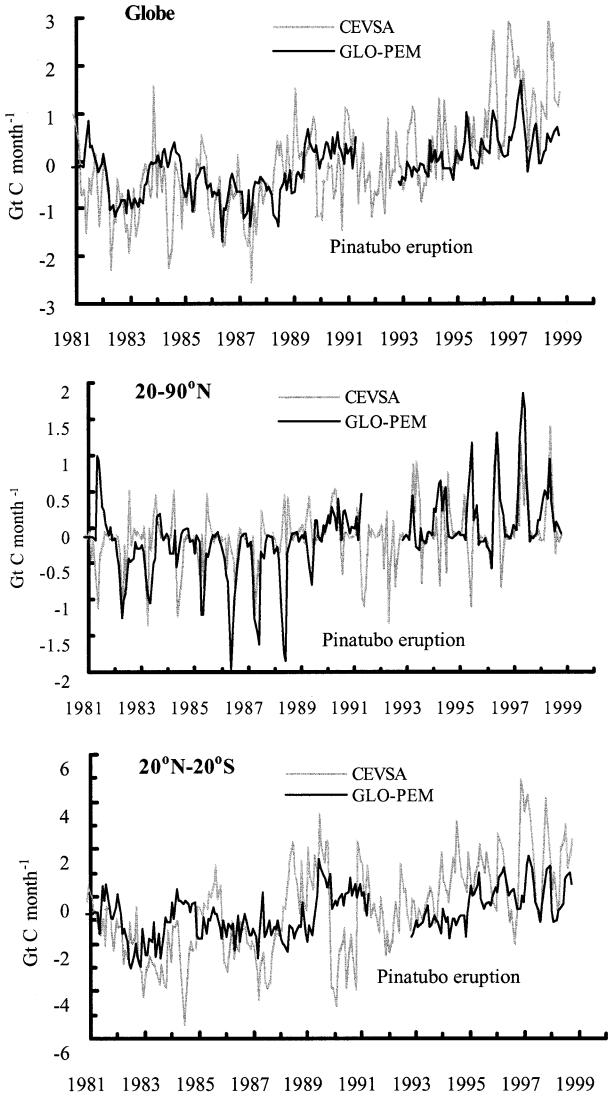

Figure 6. A comparison between interannual anomalies in net primary production (NPP) estimated with the Global Production Efficiency Model (GLO-PEM) and a biogeochemical model, CEVSA (Cao and Woodward 1998; Cao and others 2002).

Conclusions and Discussion

Our estimates showed a trend toward increasing NPP that was superimposed on high seasonal and interannual variability and similar NPP increases in the north and the tropics in 1981–2000. NPP generally decreased in El Niño seasons and increased in La Niña seasons; however, the response varied widely in individual ENSO events and in different regions. The interannual variation in NPP was cor-

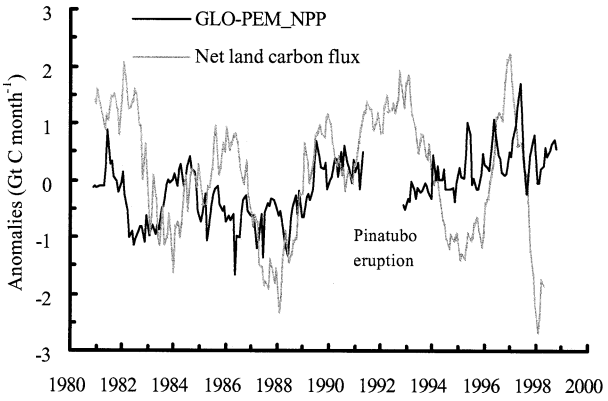

Figure 7. A comparison between the variation in net primary production (NPP) and the net terrestrial carbon uptake, as inferred from atmospheric inverse modeling (Bousquet and others 2000). The NPP increases in La Niña seasons (1983–84, 1989–90, 1996–97) and the NPP decreases in El Niño seasons (1982–83, 1987–88, and 1997–98) are consistent with the changes in terrestrial carbon uptake. Nevertheless, other processes also affect terrestrial carbon uptake; for example, its dramatic increases in 1991–93 and decreases in 1995–96 were caused by temperature-induced changes to soil heterotrophic respiration (Cao and others 2002).

related positively with temperature only in northern high latitudes (above 50°N); in other latitudinal bands, it was correlated positively with precipitation. Global NPP increases were mainly related to increases in atmospheric CO_2 and precipitation.

Our estimates are consistent with field observations and atmospheric measurements; nevertheless, they should be read cautiously. Although various calibrations and corrections were applied to the satellite data, bias arising from satellite adjustments to the multiyear data cannot be ruled out. In addition, satellite orbital degradation may cause increases of solar zenith angles and hence lead to an underestimation of NDVI and NPP for low-latitude regions (Los and others 2000; Slayback and others 2003).

We excluded the period 1991–92 from our study because of the effect of aerosols from the Pinatubo eruption, even though some investigators reported that the stratospheric aerosols probably did not reach a steady state until after the 1990s (Robock 2002). In addition, the effect of the aerosols may have caused real NPP decreases in 1991 and 1992 due to concomitant reductions in PAR and global cooling (Lucht and others 2002; Cao and others 2002), but it is difficult to separate this real effect from the interference with AVHRR observation caused by the aerosols (Slayback and others 2003).

This study is the first attempt to quantify interannual variations in NPP at the global scale using variables based almost entirely on satellite observations. The fact that our results accord with atmospheric measurements and field observations indicates that this approach has the capacity to detect NPP patterns and temporal variability realistically. The estimated spatio-temporal changes in NPP reflect the response of this important indicator of ecosystem health to global climatic phenomena such as warming, ENSO cycles, and increases in atmospheric CO_2, as well as regional climate variability. Our analysis underscores the importance of continuing global satellite observations of ecosystem changes in this critical era of rapid environmental change. To make better use of the long-term AVHRR data, further improvements are needed to remove the artifacts that may arise from various types of interference.

REFERENCES

Agbu PA, James ME. 1994, The NOAA/NASA Pathfinder AVHRR Land Data Set user's manual. Greenbelt (MD): Goddard Distributed Active Archive Center, NASA, Goddard Space Flight Center.

Asrar GM, Fuchs M, Kanemasu ET, Hatfield JL. 1984. Estimating absorbed photosynthetically active radiation and leaf area index from spectral reflectance in wheat. Agron J 87:300–6.

Barber VA, Juday GP, Finney BP. 2000. Reduced growth of Alaskan white spruce in the twentieth century from temperature-induced drought stress. Nature 405:668–73.

Battle M, Bender M, Tans PP, White JWC, Ellis JT, Conway T, Francey RJ. 2000. Global carbon sinks and their variability, inferred from atmospheric O_2 and ^{13}C. Science 287:2467–70.

Behrenfeld MJ, Randerson JT, McClain CR, Feldman GC, Los SO, Tucker CJ. 2001. Biospheric primary production during an ENSO transition. Science 291:2594–7.

Bousquet P, Peylin P, Ciais P, Le Quere C, Friedlingstein P, Tans PP. 2000. Regional changes in carbon dioxide fluxes of land and oceans since 1980. Science 290:1342–6.

Braswell BH, Schimel DS, Linder E, Moore B. 1997. The response of global terrestrial ecosystems to interannual temperature variability. Science 278:870–2.

Cao MK, Woodward FI. 1998. Dynamic responses of terrestrial ecosystem carbon cycling to global climate change. Nature 393:249–52.

Cao MK, Prince SD, Shugart HH. 2002. Effects of interannual climate variability on global terrestrial biospheric CO_2 fluxes. Global Biogeochem Cycles 16:1069, doi: 10.1029/2001GB001553.

Collatz GJ, Ball JT, Grivet C, Berry JA. 1991. Physiological and environmental regulation of stomatal conductance, photosynthesis and transpiration: a model that includes a laminar boundary layer. Agric For Meteorol 54:107–36.

Cramer W, Bondeau A, Woodward FI, Prentice IC, Betts RD. 2001. Global responses of terrestrial ecosystem structure and function to CO2 and climate change: results from six dynamic global vegetation models. Global Change Biol 7:357–73.

Czajkowski KP, Mulhern T, Goward SN, Cihlar J, Dubayah RO, Prince SD. 1997. Biospheric environmental monitoring at

BOREAS with AVHRR observations. J Geophys Res 102:29,651–62.

Dai A, Wigley TML. 2000. Global patterns of ENSO-induced precipitation. Geophys Res Lett 27:1283–6.

Davey MK, Anderson DLT. 1999. A comparison of the 1997/98 El Niño with other such events. Weather 54:295–302.

Drake BG, Gonzalez-Meler MA, Long SP. 1997. More efficient plants: a consequence of rising atmospheric CO2? Annu Rev Plant Physiol Plant Molec Biol 48:609–39.

Farquhar GD, Von Caemmerer S, Berry JA. 1980. A biochemical model of photosynthetic CO_2 assimilation in levels of C3 species. Planta 149:78–90.

Field CB, Behrenfeld MJ, Randerson JT, Falkowski P. 1998. Primary production of the biosphere: integrating terrestrial and oceanic components. Science 281:237–40.

Frouin R, Pinker RT. 1995. Estimating photosynthetically active radiation (PAR) of the Earth's surface from satellite observations. Remote Sens Environ 51:98–107.

Glantz M, Katz R, Nicholls N. 1991, Teleconnection linking worldwide climate anomalies. Cambridge (UK): Cambridge University Press.

Gleason ACR, Prince SD, Goetz SJ. 2002. Effects of orbital drift on land surface temperatures recoved from AVHRR sensors. Remote Sens Environ 79:147–65.

Goetz SJ, Prince SD. 1999. Modeling terrestrial carbon exchange and storage: the evidence for and implications of functional convergence in light use efficiency. Adv Ecol Res 28:57–92.

Goetz SJ, Prince SD, Goward SN, Thawley MM, Small J. 1999. Satellite remote sensing of primary production: an improved production efficiency modeling approach. Ecol Model 122: 235–9.

Goetz SJ, Prince SD, Small J, Gleason ACR, Thawley MM. 2000. Interannual variability of global terrestrial primary production: reduction of a model driven with satellite observations. J Geophys Res 105:20,007–91.

Gollan T, Schurr U, Shulze EC. 1992. Stomatal response to drying soil in relation to changes in the xylem sap composition of *Hhelianthus annuus:* I. The concentration of cations, anions, amino acids in and pH of, the xylem sap. Plant Cell Environ 15:551–9.

Grace J, Lloyd J, Macintyre JA, Miranda AC, Meir P. 1995. Carbon dioxide uptake by undisturbed tropical forests, 1992 and 1993. Science 270:778–80.

Gutièrrez JR. 2000. Variation in vegetation and seed bank in a Chilean semiarid community affected by ENSO 1997. J Veget Sci 11:641–8.

Gutman GG. 1999a. On the monitoring of land surface temperatures with the NOAA/AVHRR: removing the effect of satellite orbit drift. Int J Remote Sens 20:3407–13.

Gutman GG. 1999b. On the use of long-term global data of land reflectance and vegetation indices derived from the advanced very high resolution radiometer. J Geophys Res 104:6241–25.

Halpert MS, Ropelewski CF. 1992. Surface temperature patterns associated with the El Niño–Southern Oscillation. J Clim 5:577–93.

Huffman GJ, Bolvin DT. 2000, GPCP version 2 combined precipitation data set documentation. SSAI and Laboratory for Atmosphere,. Greenbelt (MD): NASA Goddard Space Flight Center.

Jarvis PG. 1976. The interpretation of the variations in leaf water potential and stomatal conductance found in canopies in the field. Philos Trans R Soc Lond B273:593–610.

Keeling RF, Piper SC, Heimann M. 1996. Global and hemispheric CO_2 sinks deduced from changes in atmospheric O_2 concentrations. Nature 381:218–21.

Keeling CD, Whorf TP. 2002. Atmospheric CO_2 records from sites in the SIO air sampling network. In: . ., Eds. Trends: a compendium of data on global change. Oak Ridge (TN): Carbon Dioxide Information Analysis Center, Oak Ridge National Laboratory. p .

Kirschbaum MUF. 1994. The sensitivity of C_3 photosynthesis to increasing CO_2 concentration: a theoretical analysis of its dependence on temperature and background CO_2 concentration. Plant Cell Environ 17:747–54.

Körner C. 2000. Biosphere responses to CO_2-enrichment. Ecol Appl 10:1590–619.

Lau KM, Wu HT. 1999. Assessment of the impacts of the 1997/98 El Niño on the Asian-Australia monsoon. Geophys Res Lett 26:1747–50.

Long SP. 1991. Modification of the response of photosynthetic productivity to rising temperature by atmospheric CO_2 concentrations: has its importance been underestimated? Plant Cell Environ 14:729–39.

Los SO, Collatz GJ, Sellers PJ. 2000. A global 9-yr biophysical land surface dataset from NOAA AVHRR data. J Hydrometeorol 1:183–99.

Lucht W, Prentice IC, Myneni RB. 2002. Climatic control of the high latitude vegetation greening trend and Pinatubo effect. Science 296:1687–9.

Malhi Y, Grace J. 2000. Tropical forests and atmospheric carbon dioxide. Trends Ecol Evol 15:332–7.

Malmström CM, Thompson MV, Juday GP, Los SO, Randerson JT, Field CB. 1997. Interannual variation in global scale net primary production: testing model estimates. Global Biogeochem Cycles 11:367–92.

Melillo JM, McGuire AD, Kicklighter DW, Moore B III, Vorosmarty CJ, Schloss AL. 1993. Global climate change and terrestrial net primary production. Nature 363:234–40.

Moron V, Ward MN. 1998. ENSO teleconnections with climate variability in the European and African sectors. Weather 53: 287–95.

Myneni RB, Keeling CD, Tucker CJ, Asrar G, Nemani RR. 1997. Increased plant growth in the northern high latitudes from 1981 to 1991. Nature 386:698–702.

Myneni RB, Dong J, Tucker CJ, Kaufmann RK, Kauppi PE, Liskki J, Zjou L, and others. 2001. A large carbon sink in the woody biomass of northern forests. Proc Nat'l Acad Sci USA 98:14784–9.

Parker DE, Horton EB. 1999. Global and regional climate in 1998. Weather 54:173–88.

Parker DE, Horton EB, Gordon M. 1998. Global and regional climate in 1997. Weather 53:166–175.

Parton WJ, Scurlock JMO, Ojima DS. 1993. Observations and modelling of biomass and soil organic matter dynamics for the grassland biome worldwide. Global Biogeochem Cycles 7:785–809.

Phillips OL, Malhi Y, Higuchi N, Laurance WF, Nunez PV, Vasquez RM, Laurance SG, and others. 1998. Changes in the carbon balance of tropical forests: evidence from long-term plots. Science 282:439–42.

Pinker RT, Laszlo I. 1992. Global distribution of photosynthetically active radiation as observed from satellites. J Clim 5:56–65.

Poliss GA, Hurd SD, Jackson CT, Piñero FS. 1997. El Niño effects

on the dynamics and control of an island ecosystem in the Gulf of Calfornia. Ecology 78:1884–97.

Potter CS, Randerson JT, Field CB, Matson PA, Vitousek PM, Mooney HA, Klooster SA. 1993. Terrestrial ecosystem production: a process model based on global satellite and surface data. Global Biogeochem Cycles 7:811–41.

Potter CS, Klooster SA, Brook V. 1999. Interannual variability in terrestrial net primary production: exploration of trend and control on regional to global scale. Ecosystems 2:36–48.

Prentice IC, Cramer W, Harrison SP, Leemans P, Monserud RA, Solomon AM. 1992. A global biome model based on plant physiology and dominance, soil properties, and climate. J Biogeog 19:117–34.

Prentice IC, Farquhar GD, Fasham MJR, Heimann ML, Jaramillo VJ, Kheshgi HS. 2001. The carbon cycle and atmospheric carbon dioxide. In Houghton JT, Ding Y, Griggs DJ, Noguer M, van der Linden PJ, Dai X, Maskell K, and others, editors. Climate change 2001: the scientific basis. Cambridge (UK): Cambridge University Press. p 183–237.

Prince SD. 1991a. Satellite remote sensing of primary production: comparison of results for Sahelian grasslands 1981–1988. Int J Remote Sens 12:1301–11.

Prince SD. 1991b. A model of regional primary production for use with coarse-resolution satellite data. Int J Remote Sen 12:1313–30.

Prince SD, Goward SN. 1995. Global primary production: a remote sensing approach. J Biogeog 22:815–35.

Prince SD, Goward SN. 1996. Evaluation of the NOAA/NASA Pathfinder AVHRR Land Data Set for global primary production modeling. Int J Remote Sen 17:217–21.

Prince SD, Goetz SJ, Dubayah RO, Czajkowski KP, Thawley M. 1998. Inference of surface and air temperature, atmospheric precipitable water and vapor pressure deficit using AVHRR satellite observations: comparison with field observations. J Hydrol 212–3:230–49.

Raich JW, Rastetter EB, Melillo JM, Kicklighter DW, Steudler PA, Peterson J. 1991. Potential net primary productivity in southern America: application of a global model. Ecol Appl 1:399–429.

Rao CRN. 1993. Degradation of the visible and near-infrared channels of the Advanced Very High Resolution Radiometer on the NOAAP9 spacecraft: assessment and recommendations for corrections. NOAA Technical Report NESDIS-70. Washington, (DC): NOAA/NESDIS.

Robock A. 2002. Pinatubo eruption: the climatic aftermath. Science 295:1242–4.

Ropelewski CF, Halpert MS. 1986. North American precipitation patterns associated with the E1 Niño–Southern Oscillation (ENSO). Monthly Weather Rev 114:2352–62.

Ropelewski CF, Halpert MS. 1987. Global and regional scale precipitation patterns associated with the E1 Niño–Southern Oscillation. Monthly Weather Rev 115:1606–26.

Rossow AB, Walker AW, Beuschel DE, Roiter MD. 1996. International Satellite Cloud Climatology Project (ISCCP) documentation of new cloud datasets. WMO/TD No. 737. World Meteorological Organization.

Rundquist BC, Harrington JA, Goodin DG. 2000. Mesoscale satellite bioclimatology. Prof Geog 52:331–44.

Schimel DS, House JI, Hibbard KA, Bousquet P, Ciais C. 2001. Recent patterns and mechanisms of carbon exchange by terrestrial ecosystems. Nature 414:169–72.

Sellers PJ, Berry JA, Collatz GJ, Field CB, Hall FG. 1992. Canopy reflectance, photosynthesis and respiration: III. A reanalysis using improved leaf models and a new canopy integration scheme. Remote Sens Environ 42:187–216.

Slayback DA, Pinzon JE, Los SO, Tucker CJ (2003) Northern hemisphere photosynthetic trends 1982–1999. Global Change Biol. 9: 1–15

Slingo J. 1999. The 1997/98 El Niño. Weather 54: 274–81, 295–302.

Stewart JB. 1988. Modeling surface conductance of pine forest. Agric For Meteorol 43:19–35.

Tardieu F, Davies WJ. 1993. Integration of hydraulic and chemical signaling in the control of stomatal conductance and water status of drought plants. Plant Cell Environ 16:341–9.

Tian H, Melillo JM, Kicklighter DW, McGuire AD, Helfrich JVK III, Moore B III, Vörösmarty CJ. 1998. Effect of interannual climate variability on carbon storage in Amazonian ecosystems. Nature 396:664–7.

Tucker CJ, Townshend JRG, Goff TE. 1985. African land-cover classification using satellite data. Science 227:369–75.

Tucker CJ, Slayback DA, Prinzon JE, Los SO, Myneni RB, Taylor MG. 2001. Higher northern latitude normalized difference vegetation index and growing season trends from 1982 to 1999. Int J Biometeorol 45:184–90.

Wilhite DA, Wood DA, Meyer SJ. 1987. Climate-related impacts in the United States during the 1982–83 El Niño. In: . ., Eds. Climate crisis. Boulder (CO): United Nation Environmental Program (Nairobi) and National Center of Atmospheric Research. p 75–8.

Wolter K, Timlin MS. 1998. Measuring the strength of ENSO—how does 1997/1998 rank. Weather 53:315–24.

Zhou L, Tucker CJ, Kaufmann RK, Slayback D, Shabanov NV, Myneni RB. 2001. Variations in northern vegetation activity inferred from satellite data of vegetation index during 1981 to 1999. J Geophys Res 106:20,069–83.